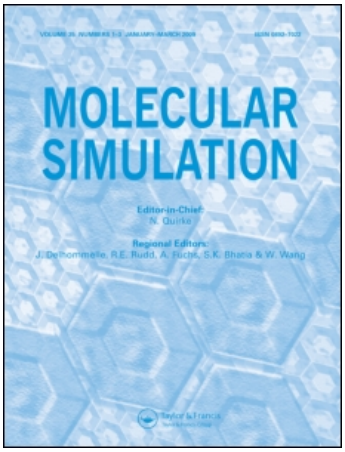

Molecular Simulation
Publication details, including instructions for authors and subscription information:
http://www.informaworld.com/smpp/title~content=t713644482

Interatomic Potentials for Simulating MnO_2 Polymorphs

Sean D. Fleming[a]; Jonathon R. Morton[a]; Andrew L. Rohl[a]; Chris B. Ward[b]
[a] A.J. Parker CRC for Hydrometallurgy, Nanochemistry Research Institute, Curtin University of Technology, Perth, WA, Australia [b] HiTec Energy Ltd, West Perth, WA, Australia

To cite this Article Fleming, Sean D. , Morton, Jonathon R. , Rohl, Andrew L. and Ward, Chris B.(2005) 'Interatomic Potentials for Simulating MnO_2 Polymorphs', Molecular Simulation, 31: 1, 25 — 32
To link to this Article: DOI: 10.1080/08927020412331298702
URL: http://dx.doi.org/10.1080/08927020412331298702

Molecular Simulation, VOL. 31 (1), 15 January 2005, pp. 25–32

Taylor & Francis
Taylor & Francis Group

Interatomic Potentials for Simulating MnO_2 Polymorphs

SEAN D. FLEMING[a], JONATHON R. MORTON[a], ANDREW L. ROHL[a,*] and CHRIS B. WARD[b]

[a]*A.J. Parker CRC for Hydrometallurgy, Nanochemistry Research Institute, Curtin University of Technology, P.O. Box U 1987, Perth, WA 6845, Australia;* [b]*HiTec Energy Ltd, P.O. Box 1597, West Perth, WA 6872, Australia*

(Received August 2004; In final form August 2004)

Interatomic potentials for manganese dioxide have been derived via fitting to the structures of the chain MnO_2 polymorphs, pyrolucite and ramsdellite. The quality of the potentials was assessed by using them to simulate the structure of spinel-based λ-MnO_2, which was not part of the fitting set. Lattice parameters of all three structures were reproduced to within 2% of the experimental values. The potentials have also been used to successfully simulate the idealised structures of the MnO_2 polymorphs containing tunnels and suggest that tunnels larger than 2 × 3 are not stable without the presence of additional species within them. The stabilities of the polymorphs have been calculated and, somewhat unexpectedly, the spinel-based structure is found to be less stable that the tunnel structures.

Keywords: Electrolytic manganese dioxide (EMD); Polymorphs; Interatomic Potentials; Molecular modelling

INTRODUCTION

Electrolytic manganese dioxide (EMD) is a form of MnO_2 that is produced via the electrolysis of Mn^{2+} solutions (usually $MnSO_4$) and is used as the primary constituent of cathodes in alkaline and button cell batteries. The structure of EMD is not well characterized and is highly disordered, but is thought to be predominantly ramsdellite, with randomly dispersed regions of pyrolusite [1]. Most postulated structural models describe EMD as an ideal ramsdellite lattice containing two kinds of defects; the first is a stacking disorder which occurs at the interface between ramsdellite and pyrolusite regions, known as de Wolff defects, and the second a micro-twinning defect, the most common of which occur on the (021) and (061) planes [2]. A large number of point defects are also known to occur in EMD; these are important to the electrochemistry, but they are of lesser importance to structural characterization [3]. Because of the high concentration of defects in EMD, some authors have classified the structure as a disordered, random intergrowth of ramsdellite and pyrolucite. Hence, EMD has been quantitatively characterized in the literature by defect concentrations, most importantly the pyrolucite concentration (P_r) and the degree of micro-twinning (T_w) that occur within the ramsdellite matrix [4]. It is this high concentration of defects that make structural characterisation of EMD so difficult. Very recently, there have been two significant modelling papers which have attempted to rationalise the structures of EMD.

Balachandran and coworkers [5] used DFT to successfully study various proposed small unit cell representations of EMD, whilst Hill *et al.* [6] used interatomic potentials to directly examine de Wolff defects and microtwinning in EMD. However, they used a generalized forcefield (CVFF), which reproduced the structures of ramsdellite and pyrolucite to within 3% and 2%, respectively.

MnO_2 has many polymorphs, which can be classified into four major groups [7]:

- Chain structures
- Spinel structures
- Tunnel structures
- Layer structures

There are two ordered chain structure polymorphs of MnO_2, pyrolusite (β-MnO_2), and ramsdellite. These chain structures consist of a slightly distorted hexagonally close packed array of oxygen ions. In pyrolucite (Fig. 1), every second row of octahedral sites is occupied by manganese ions, leading to the appearance of 1 × 1 tunnels. In contrast, ramsdellite

*Corresponding author. E-mail: andrew@power.curtin.edu.au

ISSN 0892-7022 print/ISSN 1029-0435 online © 2005 Taylor & Francis Ltd
DOI: 10.1080/08927020412331298702

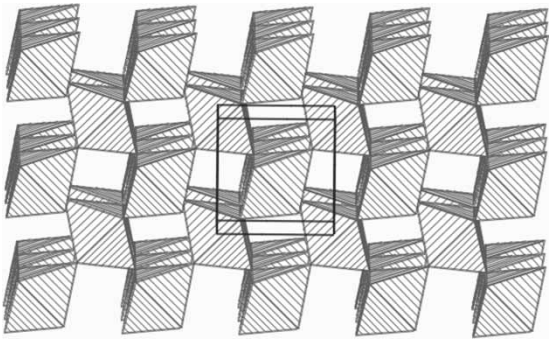

FIGURE 1 Pyrolucite Lattice viewed along the *c* axis.

(Fig. 2) has pairs of rows occupied along the c axis, leading to 2×1 tunnels.

Spinel MnO_2 (λ-MnO_2) structures have a cubic closed packed oxygen substructure, and are prepared by removing Li^+ from $LiMn_2O_4$ [8]. The manganese cations sit in the spinel octahedral sites.

MnO_2 tunnel structures are based on the structure of ramsdellite [9]. In these structures, even more rows of adjacent octahedral sites are occupied, which in turn leads to larger 3D-tunnels (Figs. 3, 5 and 7). In natural specimens, some of the Mn^{4+} is replaced by Mn^{3+}. This charge is balanced by cations such as Ba^{2+}, Pb^{2+}, Li^+, Na^+, K^+, and NH_4^+, which are located in the cavities/tunnels within these structures together with water molecules [7].

In general, layer structured manganese dioxides consist of single layers of water and/or cations sandwiched between layers of edge shared Mn octahedral [9]. As a result, structural strength is maintained by coordination and hydrogen bonding.

This study will focus on the derivation of accurate interatomic potentials, which will be fitted to the pyrolucite and ramsdellite structures and will be used in subsequent papers to model the complex structure of EMD. The quality of the potentials will be assessed by simulating the ideal Mn^{4+} only structures of the other forms of manganese dioxide. Note that the layer structured MnO_2 polymorphs are excluded from this study as the presence of species other than Mn^{4+} and O^{2-} are necessary for these structures to exist.

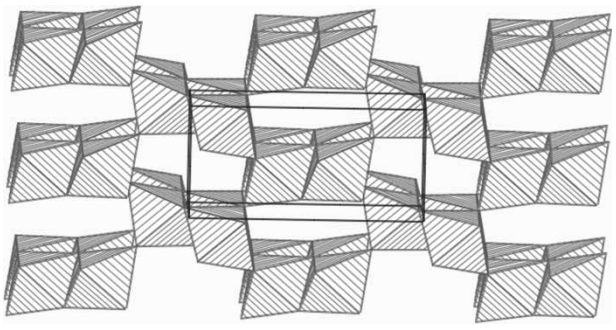

FIGURE 2 Ramsdellite lattice viewed along the *c* axis.

THEORY

A classical force field approach was employed to describe the atomic interactions in manganese dioxide. The Born model was used, which involves partitioning the lattice energy into Coulombic point charge interactions and non-Coulombic interaction terms; the latter including short-range repulsion and dispersion forces. Temperature effects were not considered. Parameterization of the force field was achieved using a least squares approach. Experimental values of the unit cell parameters and atomic positions for ramsdellite [10] and pyrolucite [11] from the literature were used in the fitting process. The computational package GULP [12] was employed in computing the minimum energy structures and to assist in the fitting stage.

The non-Coloumbic interactions were modelled using a Morse potential, which takes the form:

$$E(r) = D_e\left(1 - e^{-\alpha(r_0 - r)^2}\right)$$

with the customizable parameters D_e, α, and r_0 defining the energy contribution E for a particular pair of atoms at separation r.

A geometry dependent charge model was employed to compute the electrostatic contribution to the lattice energy, as implemented in the GULP package [12]. The method used was the charge equilibration scheme of Gordon and Rappé [13], with a modification that evaluates the analytical derivatives more efficiently [12]. Using this approach, atomic charges are assigned by solving coupled equations involving the electronegativity and the Coulombic interaction between charge sites. Evaluation of the Coulomic interaction is split into two parts; the short-range interactions (within 15 Å) are calculated by integration over two Slater s orbitals; and the long-range (beyond 15 Å) interactions are taken to be the classical Coulomb potential. The latter are evaluated using the Ewald summation technique.

POTENTIAL FITTING

The initial stage of this work was aimed at successfully modelling the crystal structures of pyrolucite and ramsdellite. This was accomplished by employing existing model parameters for manganese dioxide in the literature and adapting potentials in the literature for TiO_2. In all cases, an attempt was made to refine the potentials.

POTENTIAL TESTING

Coordinates of various MnO_2 polymorphs were taken from the ICSD database [14]. These structures

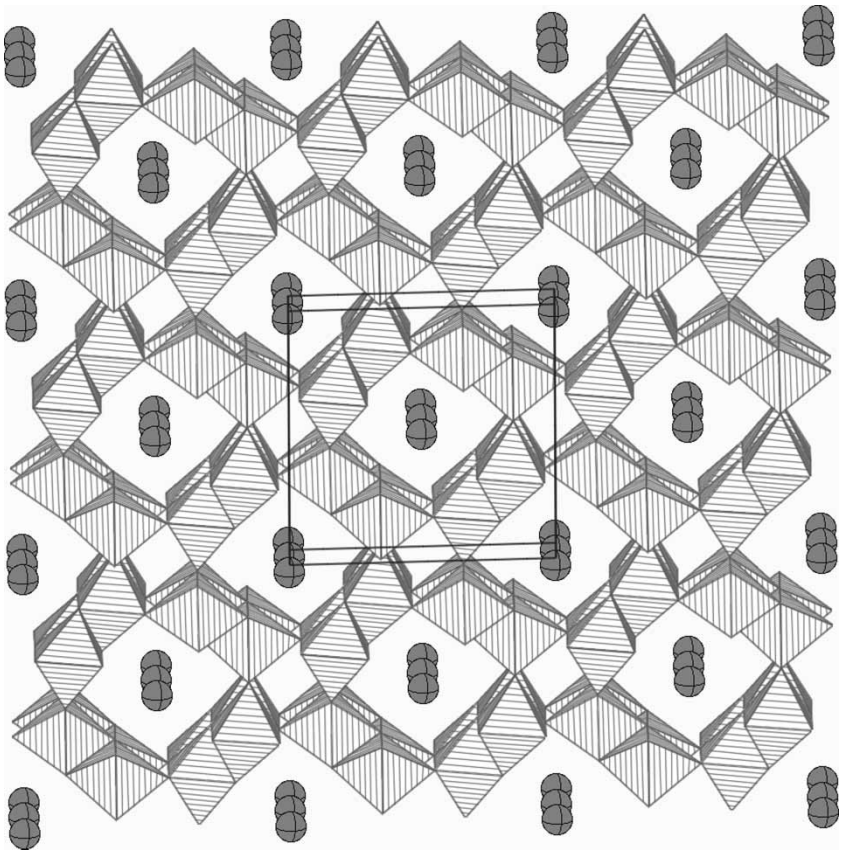

FIGURE 3 Structure of Hollandite, Coronadite and Cryptomelane viewed along the *b* axis.

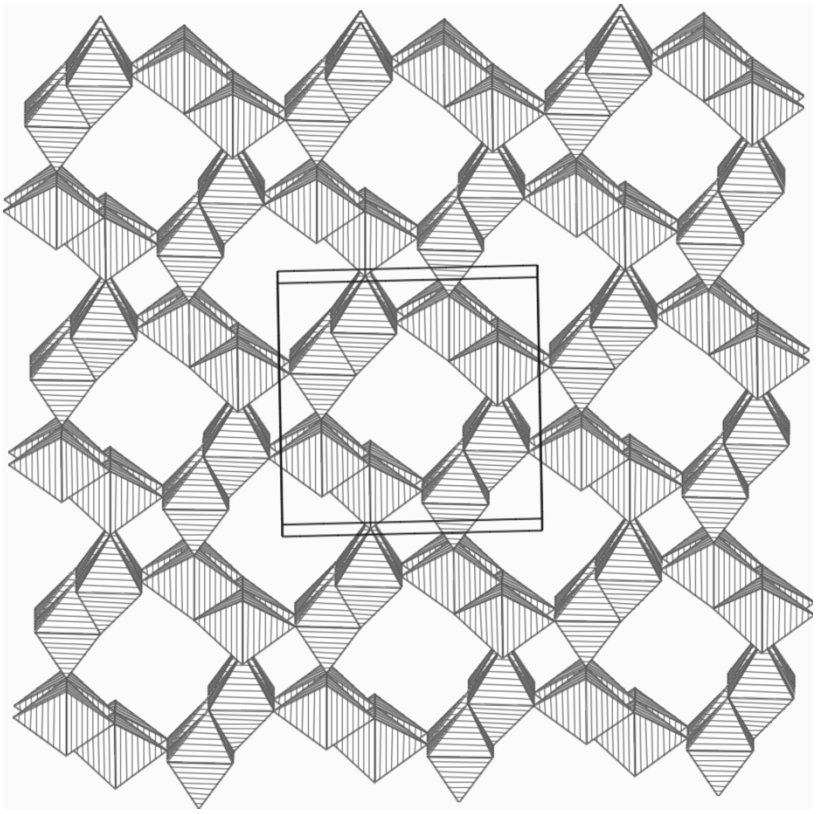

FIGURE 4 Simulated 2 × 2 tunnel structure viewed along the *b* axis.

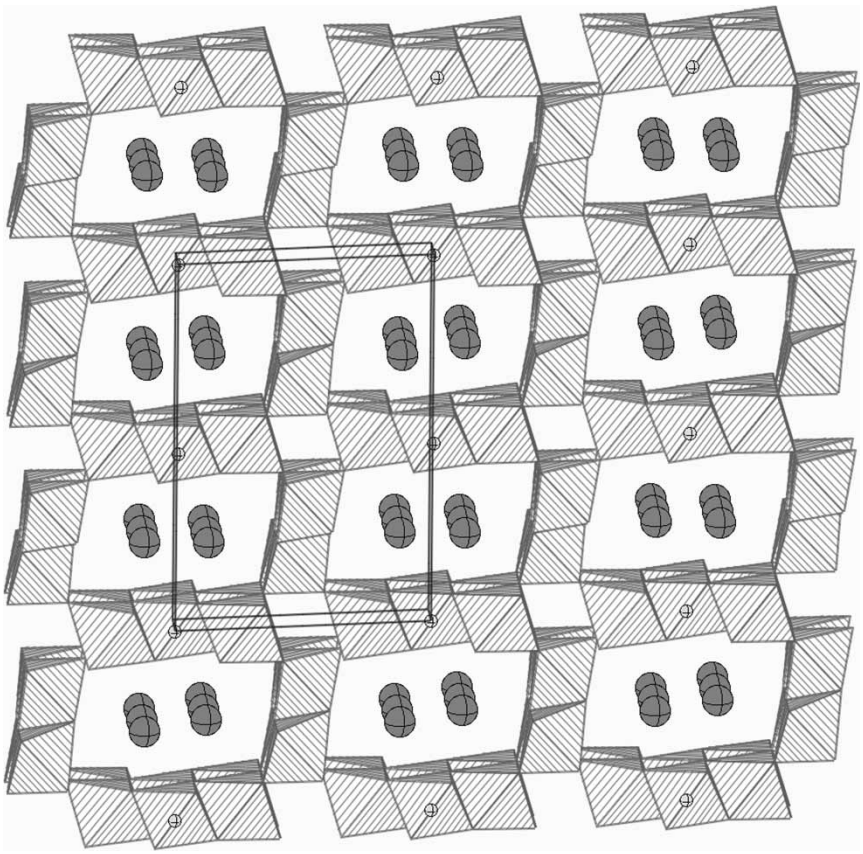

FIGURE 5 Romanechite structure viewed along the *b* axis.

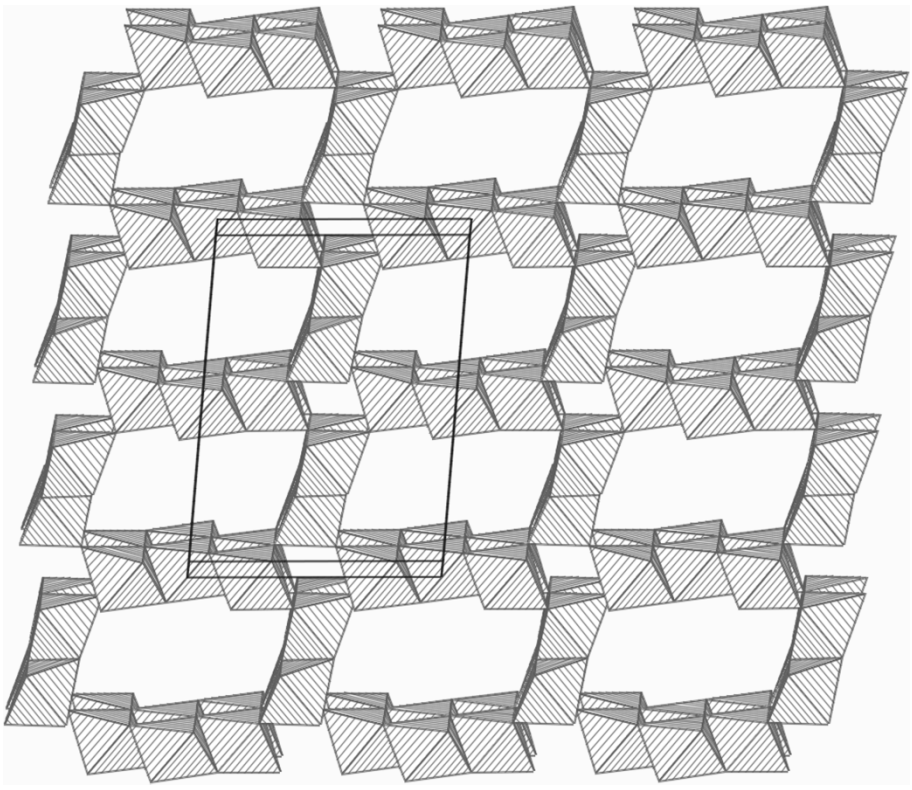

FIGURE 6 Simulated 2 × 3 tunnel structure viewed along the *b* axis.

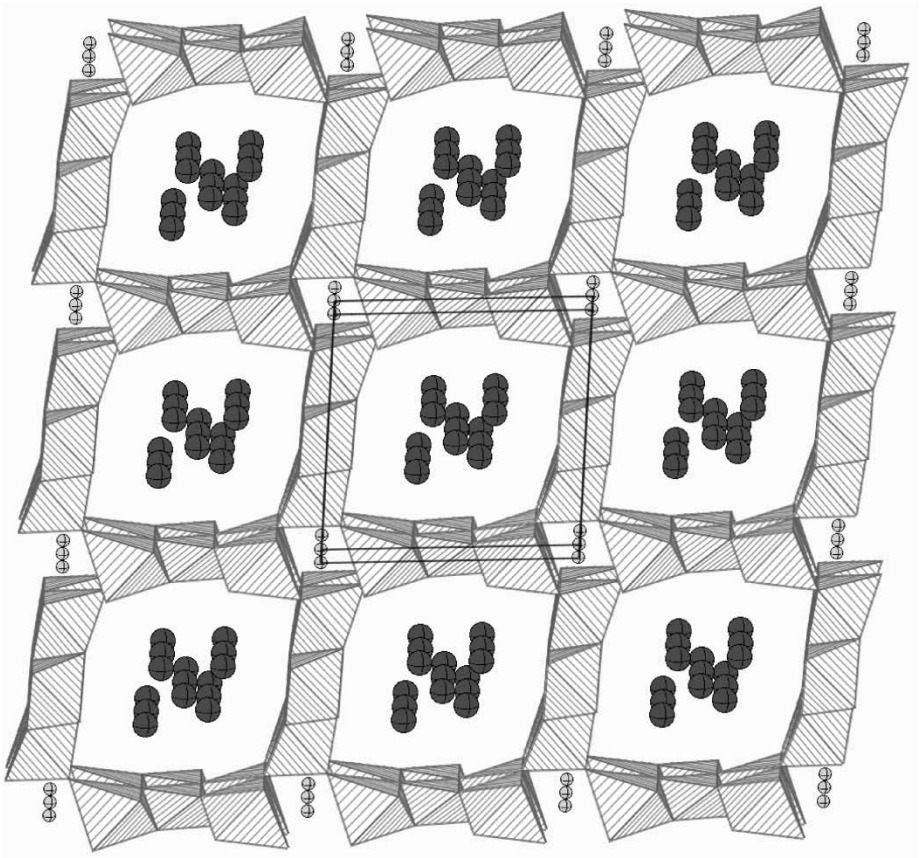

FIGURE 7 Todorokite lattice viewed along the *b* axis.

were then imported into GDIS [15]. All atoms, other than manganese and oxygen, were then removed from the crystal structure, and the structure optimized by GULP using the potentials derived for ramsdellite and pyrolusite earlier and the changes in structure observed. Since the counter ions in the experimental structures were removed, all the manganese ions are in the +4 oxidation state. The polymorphs modeled were:

- Chain structures (ramsdellite and pyrolusite)
- 2 × 2 tunnel structures (hollandite, corondite and crytomelane)
- 2 × 3 tunnel structures (romanechite)
- 3 × 3 tunnel structures (todorokite)
- Spinel structures ($LiMn_2O_4$)

RESULTS/DISCUSSION

Potential Fitting

Ramsdellite and Pyrolucite

The initial stage of this work was aimed at successfully modelling the crystal structures of pyrolucite and ramsdellite. This was accomplished by employing existing model parameters for manganese dioxide in the literature [16,17], and adapting previously published potentials for rutile [18,19] and anatase [20]. A distinguishing characteristic of the two manganese dioxide models is that one employs a shell mode for oxygen [17], whilst the other does not [16]. The best result was derived from the variable charge model of Swamy *et al.* [19], with the final interatomic parameters given in Table I.

The quality of the derived potentials was judged by how well they reproduce the crystal structures of pyrolucite and ramsdellite (Figs. 1 and 2). Note that an attempt was made to modify all potential parameters from their original form, since some were originally intended for non-manganese dioxide systems. Unsurprisingly, in the case of the two manganese dioxide models, no better result than the original values could be found. In Table II, we present the best results that were obtained in this study for each of the derived potential models.

TABLE I The fitted parameters for the Morse potentials in the variable charge model developed for simulating the structures of pyrolucite and ramsdellite

	D_e (eV)	a ($Å^{-1}$)	r_0 (Å)
Mn–O	1.09069	3.98071	1.78017
Mn–Mn	0.005645	1.69722	4.14158
O–O	0.041159	1.16724	3.69663

TABLE II The percentage errors between the calculated and the experimental lattice parameters of pyrolusite [10] and ramsdellite [11] for the fitted potential models derived from the literature

	Pyrolusite			*Ramsdellite*		
Original publication	*a*	*b*	*c*	*a*	*b*	*c*
Swamy *et al.* [19]	−0.54	−0.54	0.63	−1.32	0.92	1.74
Woodley *et al.* [16]	−2.54	−2.54	2.77	−2.11	7.08	4.53
Woodley *et al.* [17]	−2.28	−2.28	−1.41	−4.82	5.92	0.25
Sayle *et al.* [18]	−2.25	−2.25	−1.43	−4.83	5.91	0.25
Bush *et al.* [20]	−3.46	−3.46	3.39	−1.74	1.18	3.77

The high quality of our variable charge model is evident from the fact that all calculated values differ from the experimental values by less than 2%; this is the only model for which such a result was obtained. In addition, the reason for the closeness between the Woodley *et al.* [17] and Sayle *et al.* [18] result is due to the high degree of similarity between the point charges used for the atomic species.

2 × 2 *Tunnel Structures*

The Hollandite, Coronadite and Cryptomelane structures (Fig. 3) have very similar structures, the only difference being the cations that balance the Mn^{3+} in the structure. Thus, once the guest cations are removed (Fig. 4), we would expect all three manganese dioxide frameworks to converge to the same result. Table III shows that this is not the case.

In fact, two different structures are obtained, Hollandite and Cryptomelane remain monoclinic, but Coronadite converges to a tetragonal structure. In agreement with the rules of Kitaigorodsky [24], the lower symmetry structure is more stable; however the difference is very small, that is 2.148×10^{-4} eV/mol. This would certainly suggest that the monoclinic and tetragonal structures would both be expected to form, and may explain why these

TABLE III Comparison between experimental and calculated lattice parameters of hollandite, coronadite, and cryptomelane

	Parameters			
	a (Å)	*b* (Å)	*c* (Å)	*β* (Å)
Hollandite–$Ba_x(Mn^{4+},Mn^{3+})_8O_{16}$				
Experimental [21]	10.0060	2.8660	9.7460	91.17
Calculated	9.6906	2.8977	9.5709	90.28
Difference (%)	−3.15	1.11	−1.08	−0.98
Coronadite–$Pb_x(Mn^{4+},Mn^{3+})_8O_{16}$				
Experimental [22]	9.9380	2.8678	9.8340	90.39
Calculated	9.6332	2.8978	9.6295	90.01
Difference (%)	−3.07	1.05	−2.08	−0.42
Cryptomelane–$K_x(Mn^{4+},Mn^{3+})_8O_{16}$				
Experimental [23]	9.9560	2.8705	9.7060	90.95
Calculated	9.6935	2.8977	9.5676	90.29
Difference (%)	−2.64	0.95	−1.43	−0.73

TABLE IV Comparison between initial and final lattice parameters of romanechite

	Parameters			
Romanechite– $BaMn_9O_{16}(OH)_4$	*a* (Å)	*b* (Å)	*c* (Å)	*β* (°)
Experimental [25]	9.5600	2.8800	13.8500	92.50
Calculated	9.5197	2.8958	13.1523	95.03
Difference (%)	−0.42	0.55	−5.04	2.73

structures have been reported in both tetragonal and monoclinic settings, although reports of the former may be due to the limited accuracy of the X-ray machines of the time.

In all three cases, the *a* and *c* parameters shrink appreciably on removal of the counter-ions, whilst the *b* parameter lengthens. This demonstrates that the large counter-ions expand the dimensions of the channels but act to contract the cell axis along the length of the channels.

2 × 3 *Tunnel Structures*

Table IV shows that the derived interatomic potentials also satisfactorily model the 2 × 3 tunnel structure of romanechite (Figs. 5 and 6). Again the cross section of the channels shrinks upon removal of the counter-ions, whilst the axis parallel to the channels expands.

3 × 3 *Tunnel Structures*

Efforts to model the tunnel structure of todorokite were unsuccessful as the tunnels always collapsed. This was not an entirely unexpected result. Todorokite is known to convert from the tunnel to the layer configuration under certain conditions [7], thus when the species contained within the tunnels are removed, it is highly probable that the tunnel structure will collapse (Fig. 7).

Spinel Structures

Although spinel MnO_2 structures such as $LiMn_2O_4$ (Fig. 8) have little relevance to the structure of EMD as they are based on a cubic close packed oxygen substructure, they provide a good test for the quality of the potentials, as cell parameters for the pure MnO_2 polymorph are available. The results (Table V and Fig. 9) show the high quality of the potentials as the lattice parameter matches to within 1.1%. For comparison, applying the CVFF forcefield utilized by Hill and coworkers [6] yields a cell which is 3.5% larger than experiment.

Stability of the Polymorphs

The calculated stabilities of the polymorphs are listed in Table VI and clearly show that pyrolucite is the most stable polymorph, in agreement with

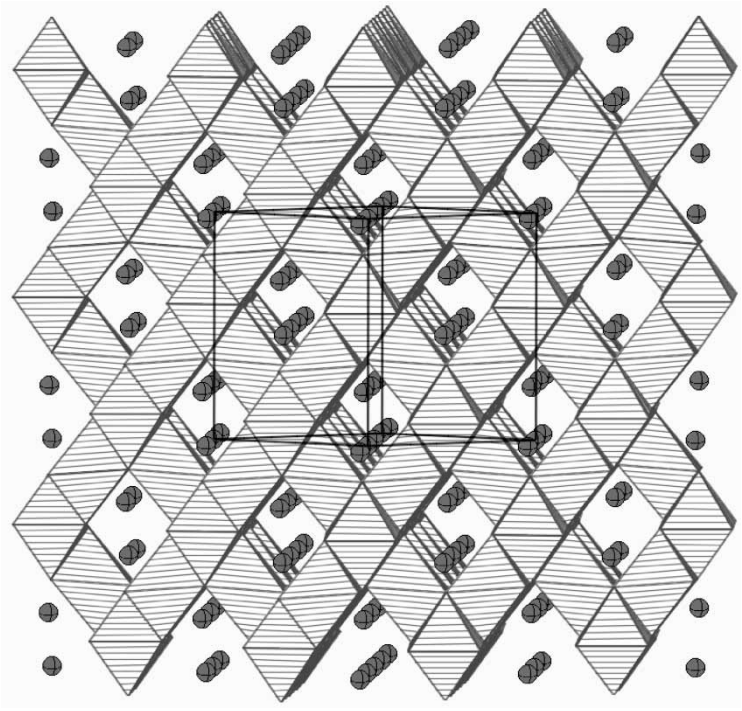

FIGURE 8 Spinel structure ($LiMn_2O_4$) viewed along *ab*.

experimental results [28]. Ramsdellite is the next most stable polymorph and these two polymorphs are substantially more stable than the rest. As expected, the stability of the tunnel structures decreases as the tunnel size increases. The most surprising result is that the spinel-based structure is the least stable.

CONCLUSION

The potentials for manganese dioxide derived in this study are of high quality as they correctly predict the lattice constants of pyrolucite, ramsdellite and λ-MnO_2 to within 2% of the experimental values. It is noteworthy that λ-MnO_2 was not included in

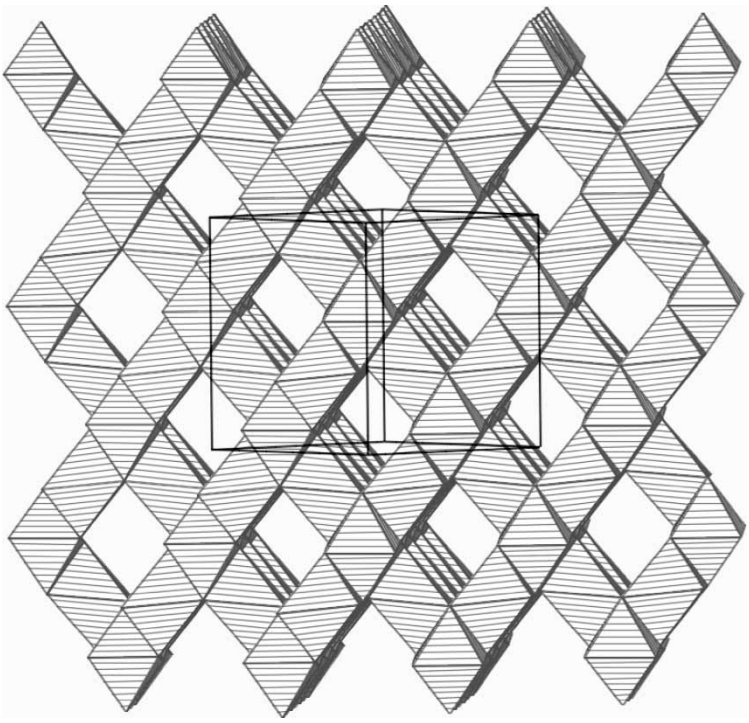

FIGURE 9 Simulated spinel structure viewed along *ab*.

TABLE V Comparison between initial and final lattice parameters of Spinel structures $LiMnO_2O_4$ and λ-MnO_2

	Parameters		
Spinel–$LiMn_2O_4$/λ-MnO_2	*a (Å)*	*b (Å)*	*c (Å)*
$LiMn_2O_4$ experimental [26]	8.2363	8.2363	8.2363
λ-MnO_2 experimental [27]	8.0290	8.0290	8.0290
Calculated	8.1172	8.1172	8.1172
λ-MnO_2 difference (%)	1.10	1.10	1.10
$LiMn_2O_4$ difference (%)	−1.45	−1.45	−1.45

TABLE VI Calculated stabilities of various MnO_2 polymorphs

Structure	*Stability (eV/mol)*
Pyrolucite	−7.072
Ramsdellite	−6.914
Hollandite	−6.680
Coronadite	−6.680
Cryptomelane	−6.680
Romanechite	−6.526
Spinel	−6.524

the fitting set. The potentials have also been found to model the idealised structures of the polymorphs containing tunnels and suggest that tunnels larger than 2×3 are not stable without the presence of additional species within them. The calculated stabilities follow expected trends and the spinel-based structure is found to be the least stable polymorph.

References

[1] Wyckoff, R.W.G. (1963) *Crystal Structures* (Wiley, New York).
[2] Pannetier, J. (1994) "Characterization of manganese dioxides by X-ray diffraction", *Prog. Batteries Battery Mater.* **13**, 132.
[3] Donne, S.W. (2000) "Alkaline manganese dioxide electrochemistry", *ITE Lett. Batteries New Technol. Med.* **1**, 915.
[4] Chabre, Y. and Pannetier, J. (1995) "Structural and electrochemical properties of the proton/γ-MnO_2 system", *Prog. Solid State Chem.* **23**, 1.
[5] Balachandran, D., Morgan, D., Ceder, G. and van de Walle, A. (2003) "First-principles study of the structure of stoichiometric and Mn-deficient MnO_2", *J. Solid State Chem.* **173**, 462.
[6] Hill, J.-R., Freeman, C.M. and Rossouw, M.H. (2004) "Understanding γ-MnO_2 by molecular modeling", *J. Solid State Chem.* **177**, 165.
[7] Williams, R.P. (1995) "Characterisation and production of high performance electrolytic manganese dioxide for use in primary alkaline cells", PhD Thesis, Department of Chemistry, The University of Newcastle.
[8] Hunter, J.C. (1981) "Preparation of a new crystal form of manganese dioxide λ-MnO_2", *J. Solid State Chem.* **39**, 142.
[9] Burns, R.G. and Burns, V.M. (1975) In: Kozawa, A. and Brodd, R.J., eds., *The Manganese Dioxide Symposium, Cleveland*, Vol. 1, 306.
[10] Fong, C., Kennedy, B.J. and Elcombe, M.M. (1994) "A powder neutron diffraction study of λ and γ manganese dioxide and of $LiMn_2O_4$", *Z. Kristallogr.* **209**, 941.
[11] Baur, W.H. (1976) "Rutile-type compounds. V. Refinements of MnO_2 and MgF_2", *Acta Crystallogr.* **B32**, 2200.
[12] Gale, J.D. and Rohl, A.L. (2003) "The General Utility Lattice Program (GULP)", *Mol. Simul.* **29**, 291.
[13] Rappe, A.K. and Goddard, W.A. III (1991) "Charge equilibration for molecular dynamics simulations", *J. Phys. Chem.* **95**, 3358.
[14] (1999) "Inorganic Crystal Structure Database (ICSD)", FIZ and Gmelin-Institute.
[15] GDIS, http://gdis.sourceforge.net and Fleming, S.D. and Rohl, A.L. "GDIS: A visualization program for molecular and periodic systems", *Z. Kristallogr.*, in press.
[16] Woodley, S.M., Battle, P.D., Gale, J.D. and Catlow, C.R.A. (1999) "The prediction of inorganic crystal structures using a genetic algorithm and energy minimisation", *Phys. Chem. Chem. Phys.* **1**, 2535.
[17] Woodley, S.M., Catlow, C.R.A., Piszora, P., Stempin, K. and Wolska, E. (2000) "Computer modeling study of lithium ion distribution in quaternary Li-Mn-Fe-O spinels", *J. Solid State Chem.* **153**, 310.
[18] Sayle, D.C., Catlow, C.R.A., Perrin, M.A. and Nortier, P. (1995) "Computer simulation study of the defect chemistry of rutile TiO_2", *J. Phys. Chem. Solids* **56**, 799.
[19] Swamy, V., Gale, J.D. and Dubrovinsky, L.S. (2001) "Atomistic simulation of the crystal structure and bulk moduli of TiO_2 polymorph", *J. Phys. Chem. Solids* **62**, 887.
[20] Bush, T.S., Gale, J.D., Catlow, C.R.A. and Battle, P.D. (1994) "Self-consistent interatomic potentials for the simulation of binary and ternary oxides", *J. Mater. Chem.* **4**, 831.
[21] Miura, H. (1986) "The crystal structure of hollandite", *Mineral. J. (Japan)* **13**, 119.
[22] Post, J.E. and Bish, D.L. (1989) "Rietveld refinement of the coronadite structure", *Am. Mineral.* **74**, 1989.
[23] Post, J.E., Dreele, R.B.V. and Buseck, P.R. (1982) "Symmetry and cation displacement in hollandites: structure refinements of hollandite, cryptomelane and priderite", *Acta Crystallogr.* **B38**, 1056.
[24] Kitaigorodsky, A.I. (1973) *Molecular Crystals and Molecules* (Academic Press, New York).
[25] Wadsley, A.D. (1953) "The crystal structure of psilomelane", *Acta Crystallogr.* **6**, 433.
[26] Cho, N.W., Chang, S. and Sung, H.P. (1997) "Synthesis and crystal structure refinement of Li (Mn-d) Ti (d) O4", RIST Yongu Nonmun (RIST Research Papers) 11, 622.
[27] Mosbah, A., Verbaere, A. and Tournoux, M. (1983) "Lithium manganate ($Li_xMnO_{2\lambda}$ phases intercalated in the spinel type", *Material. Res. Bull.* **18**, 1375.
[28] Pannetier, J. (1992) "A comprehensive structural model of EMD and CMD based on De Wolff disorder and microtwinning", *Prog. Batteries Battery Mater.* **11**, 51.